

OMS: A computer algorithm to develop closed-form solutions to multicoupled, multiphysics problems

Patricio F. Mendez*

Department of Chemical and Materials Engineering
University of Alberta
9107 116th St., Edmonton, Alberta T6G 2V4, Canada

Nicolas Stier†

Columbia Business School
Columbia University
3022 Broadway, New York, NY 10027, USA

Abstract

Typical computer code for the analysis of complex problems works by approximating the exact solution to the governing equations for a particular set of parameters. This paper discusses the OMS algorithm and its application to recirculating thermocapillary flows in the weld pool. The OMS algorithm is the implementation of the Order of Magnitude Scaling methodology, which is a radically different approach in which the computing effort results in formulae valid for any parameter value within a well-defined range. The methodology does not involve meshing and presents no convergence problems; instead, it is based on a mathematical framework that can automatically estimate characteristic values for asymptotic extremes. Because the asymptotic regime of the problem of interest is not known beforehand, the code exhausts all possible iterations

*Corresponding author: Address: Department of Chemical and Materials Engineering, University of Alberta, ECERF W7-092 9107 116th St., Edmonton, AB T6G 2V4, Canada; phone: 780 248-1587; e-mail: pmendez@ualberta.ca

†e-mail: stier@gsb.columbia.edu

between dominant forces and makes selections based on self-consistency. This approach combines elements of artificial intelligence, asymptotic analysis, and linear algebra. In addition to closed-form expressions for characteristic values, it also provides a unique set of dimensionless groups that can be used as a basis for regression analysis in calibrations against experiments. The OMS algorithm has been implemented in prototype form in Matlab and applied to the analysis of thermocapillary driven flows where 2,486 combinations of driving forces are tested, identifying 1,897 incompatible balances, 544 inconsistent balances, and 45 self-consistent balances. The 45 self-consistent balances are grouped into 14 classes, and finally the 14 classes are filtered into a single final set of closed-form expressions for maximum velocity, pressure differential, and maximum temperature. The widely accepted solutions obtained by others in the past are reproduced automatically. The potential for the treatment of more complex problems and the limitations of the methodology are discussed.

1 Introduction

This paper discusses a novel procedure called Order of Magnitude Scaling (OMS) which aims at finding the minimal representation of engineering problems based on detailed analysis of the governing equations. The methodology is based on linear algebra operations that enable the computer implementation of scaling analysis of non-linear partial differential equations, and is described in detail in [1]. In the context of OMS, scaling means assigning a characteristic value to a variable. For example, if the variable is the temperature of a fluid, which depends on space and time, the scale is typically the maximum, minimum, or average temperature within the time and space limits of interest. Characteristic values are described

in detail in [2].

The OMS algorithm applies to equations of the form:

$$\sum_j A_j f_j(\{X\}, \{U\}, \{P\}) = 0 \quad (1)$$

where f_j are functions in which the arguments are dimensionless combinations of the independent variables, the dependent variables, the parameters, and numerical constants (represented here as column vectors $\{X\}$, $\{U\}$, $\{P\}$, $\{K\}$ respectively. These sets are defined in detail in [2]. The equations can be linear or non-linear. The coefficients A_j have the form of a power law based only on the parameters of the governing equations:

$$A_j = K_j \prod_k P_k^{a_{jk}} \quad (2)$$

with K_j being a dimensionless numerical constant (for example the numbers 2 or π , or a power law of convenient numbers) and a_{jk} being the exponent of parameter k in coefficient j , typically an integer or the ratio of small integers. The parameters are always defined as positive, but functions f_j can have any sign. Expressions that do not have a power-law form can often be reduced to the form of Equation 1 [2].

1.1 Literature Review

Scaling techniques based on governing equations have been developed by many researchers in a broad spectrum of disciplines. In chemical engineering, scaling is essential for relating pilot plants to full-scale plants, and scaling techniques have been developed by Krantz [3], Sides [4], Deen [5], Astarita [6], Ruckenstein [7], Denn [8], and Aris [9]. In mechanical engineering, scaling has been used to generalize results, typically in heat transfer and fluid mechanics,

with scaling techniques developed by Bejan [10], Chen [11], Kline [12], and Rivas [13]. In materials engineering, scaling is typically used to simplify multicoupled, multiphysics problems, typically based on transport equations, such as in the books on materials processing by Dantzig and Tucker [14], Kou [15], Poirier and Geiger [16], and Szekely and Themelis [17]. Asymptotic techniques from applied mathematics have provided the foundation to much of the work on scaling in engineering through the study of order of magnitude of terms, dominant balance, and self consistency. Especially relevant is the work of Segel on self-consistency [18], VanDyke on perturbations [19], Bender and Orszag [20] and White [21] on dominant balance, and Friedrichs, Kruskal [22], Fowler [23], and Andrianov [24] on asymptotic behavior; in all these cases, the scaling approach depends on neglecting small terms in the governing equations. However, the choice of small terms in the governing equations is a significant challenge and typically involves a degree of subjectivity: “In practice each theoretician seems to dial one or more quantities to a small value in his own work and then attacks other theorists for performing unnatural acts when they do the same thing” [25]. The work presented here aims at overcoming this undesirable subjectivity by considering all relevant possibilities of small parameters with an exhaustive approach. This approach requires a computer algorithm for problems beyond the very simple, and this paper is one of the first attempts at building such algorithm using the governing equations as the starting point.

Algorithmic implementations of scaling have typically been based on dimensional analysis [26–30], or on artificial intelligence heuristics [31–37]. Only one algorithmic implementation of scaling based on governing equations has been presented before: Asymptotic Order of Magnitude (AOM) by Yip [38]. The methodology presented here is similar to AOM in

that both approaches are based on dominant balance, self-consistency, and a combinatorial exploration of possible dominant terms. The main difference between AOM and the methodology presented here is that AOM is based on an artificial intelligence approach, while this work is based on linear algebra and characteristic values; in particular, AOM starts with the equations already normalized, and the normalization does not change with the different iterations. Also, the differential expressions are not normalized by their characteristic values and can have orders of magnitude different than 1. Another important difference is that in AOM the simplifications are made on a sequential way; this has the advantage of allowing multiple term balances, but prevents the algorithm from taking advantage of the power-law form of the coefficients in the normalized equations. AOM thus results in a set of simplifications that require the solution of a non-linear set of algebraic equations. In OMS the scaling laws result from solving a system of simultaneous linear algebraic equations, since the balances considered are only between two terms. The solution of a linear system does not mean that the original governing equations have been linearized, it means that the non-linear dependences are captured in the exponents of the power-law coefficients, which become linear expressions when using logarithms. Multiple-term balances are outside the scope of this paper, but can be tackled with OMS using a relaxation technique that will be considered in a separate publication. The earliest version of OMS was introduced in [39].

1.2 Comparison of OMS with other scaling approaches based on the governing equations

All scaling approaches mentioned above are based on the governing equations and share the same conceptual core in their procedure, which is summarized in Table 1. This table also compares the OMS approach with typical manual scaling approaches.

Steps 1 to 3 in Table 1 were studied in detail in [2], and Steps 4 to 7 in [1]. In addition to the ability of being implemented as a computer algorithm, OMS has additional differences with other scaling approaches such as the typical approach based on the governing equations, dominant balance, Lie algebras, the use of ratios of forces, dimensional analysis, and inspectional analysis.

Scaling approaches based on the governing equations often suggest to solve for the unknown characteristic values (Step 5) by picking a single dominant term that includes it, and making its coefficient equal to 1 (for example [14]). This approach is insufficient for multiple coupled governing equations, where the dominant coefficients typically involve more than one unknown characteristic value, resulting in a system of multiple algebraic equations. A commonly used approach in this situation is the use of experimental or numerical data as upper or lower bound estimates for all but one unknown in each coupled equation. Although effective, this approach requires redundant additional information that is not always available or reliable.

The method of dominant balance from applied mathematics is typically applied to single equations, with the simplified equation being solved exactly. In contrast, in OMS multiple coupled equations are possible, although only characteristic values are estimated. The main

Table 1: Sequence of operations in a typical scaling approach based on governing equations

	Typical scaling approach	OMS approach
Step 1	Write the governing equations including boundary and initial conditions.	same
Step 2	Normalize the dependent and independent variables using their characteristic values. Some characteristic values might be unknown. This step results in dimensionless differential expressions based on the normalized variables.	Normalize each <i>term</i> by its characteristic value
Step 3	Insert normalized expressions into governing equations.	same
Step 4	Normalize each governing equation using the coefficient of the term expected to be dominant.	same
Step 5	Solve for the unknown characteristic values by choosing terms where they are present and making their coefficients equal to 1.	Solve system of simultaneous linear equations.
Step 6	Verify that the terms not chosen are not larger than one.	same
Step 7	If any term is larger than one, then normalize equations again assuming different dominant terms.	same

difference with the scaling analysis developed by Barenblatt [40, 41] and scaling based on Lie algebras [42] is that the scaling factors used in OMS describe characteristic values as a function of the problem parameters, not as a function of the independent variables.

Compared to the scaling approaches based on *ad hoc* dimensionless ratios of forces, OMS has the advantage that the scaling factors obtained can converge to the exact solution or very close to it because OMS takes geometrical factors and other numerical constants into account.

Inspectional analysis is a technique that generates dimensionless groups from the governing equations [43]. In inspectional analysis, it is not required that the magnitudes that normalize the variables represent characteristic values; thus, the resulting normalized governing equations do not necessarily provide representative estimates of the relative magnitude of each term.

In dimensional analysis [44] and its modern implementations [45–50], there are no guidelines for the choice between different sets of independent dimensionless groups. In contrast, in OMS the dimensionless groups generated are not arbitrary as in dimensional analysis, instead, they aim at capturing the order of magnitude of the terms of the governing equations.

The concepts and linear algebra operations developed in this work are illustrated using a detailed example involving thermocapillary flows in welding to demonstrate the capability of OMS to yield scaling laws and insight in more complex problems.

2 Mathematical background of OMS

2.1 The Matrix of Coefficients

The matrix of coefficients $[C]$ enables the automation of scaling [51]. This matrix synthesizes the engineering judgement used in Steps 1 to 3, and enables the use of linear algebra operations to implement Steps 4 to 7 as a computer algorithm.

The power law coefficients of a set of equations can be written in a general form as:

$$(C) = [C] \left\{ \begin{array}{l} (K) \\ (P) \\ (S) \end{array} \right\} \quad (3)$$

where $[C]$ is the matrix of coefficients, with a structure illustrated in Figure 1. The notation is explained in detail in Appendix A. The matrix of coefficients considers p governing equations, of which equation j has t_j coefficients. The horizontal lines divide the groups of coefficients corresponding to each governing equation. The total number of coefficients is t . The vertical lines divide the matrix in three submatrices. The leftmost submatrix (set $\{K\}$) is associated with the numerical constants that appear in the coefficients (e.g. 2, π , etc.). The submatrix in the middle contains the n columns associated with the parameters (set $\{P\}$). The submatrix on the right contains the q columns associated with the unknown characteristic values (set $\{S\}$). Following the naming convention described in Appendix A, these submatrices are named $[C]_K$, $[C]_P$, and $[C]_S$ respectively.

	K_1	\dots	K_u	P_1	\dots	P_n	S_1	\dots	S_q
$C_{1,1}$	\cdot	\dots	\cdot	\cdot	\dots	\cdot	\cdot	\dots	\cdot
\vdots	\vdots	\ddots	\vdots	\vdots	\ddots	\vdots	\vdots	\ddots	\vdots
C_{1,t_1}	\cdot	\dots	\cdot	\cdot	\dots	\cdot	\cdot	\dots	\cdot
\dots	\dots	\dots	\dots	\dots	\dots	\dots	\dots	\dots	\dots
$C_{p,1}$	\cdot	\dots	\cdot	\cdot	\dots	\cdot	\cdot	\dots	\cdot
\vdots	\vdots	\ddots	\vdots	\vdots	\ddots	\vdots	\vdots	\ddots	\vdots
C_{p,t_p}	\cdot	\dots	\cdot	\cdot	\dots	\cdot	\cdot	\dots	\cdot

Figure 1: Structure of the Matrix of Coefficients $[C]$. Line $C_{j,k}$ represents coefficient k in equation i , and each column represents a numerical constant (K_1, K_2, \dots), a problem parameter (P_1, P_2, \dots), or an unknown characteristic value (S_1, S_2, \dots) [1]

2.2 Modified Dominant Balance

The estimation of unknowns using matrix operations corresponds to Step 5 of the typical scaling procedure described in Table 1. To accomplish this, OMS follows a rigorous approach based on a modified implementation of the dominant balance technique.

Traditionally, dominant balance has three steps: 1) elimination of a term of a differential equation assuming it does not affect its asymptotic behavior; 2) solution of the simplified equation, 3) replacing the simplified solution into the original equation and verifying that the neglected term is indeed negligible [18–22, 38]. Because the verification is performed using the solution of the simplified equation, not the exact solution, there is no fail-proof bound for the errors. Self-consistency is widely used by engineers and applied mathematicians, and “pathological” cases are rare in engineering [8, 12, 18, 20]. Appendix B discusses such cases

through an example.

In the modified implementation of dominant balance in OMS, the terms are balanced by considering only their normalized characteristic values and discarding all but two terms, resulting in power-law equations, much faster to solve than a differential equation.

2.2.1 Use of characteristic values to perform balances

OMS estimates the magnitude of every term by considering only its power-law coefficients. This is also standard practice in engineering analysis [11–14], and has been studied in detail in [2]. A significant advantage of this approach is that it enables estimating the characteristic values of the unknown functions without integrating the differential equations. This is possible because the coefficients do not involve the independent variables.

Two conditions are necessary for a meaningful use of characteristic values. First, the terms considered must balance each other over almost all the domain (except at singularities). Second, the dominant terms being balanced must have their characteristic values evaluated at the same point in the domain, especially when the terms considered involve singularities.

The first condition is the “orthodoxy” condition described in [52], and provides guidelines for the division into subdomains. Subdomains should not be too large as to involve more than one pair of terms balancing each other, yet subdomains should be large enough to allow the estimation of differential expressions based on characteristic values. The presence of singularities in stiff equations is disclosed in Appendix B. From this point forward, when referring to a domain or subdomain, it will be implicit that the region surrounding a singularity is excluded.

2.2.2 Two-term balances

In applied mathematics, after removing a negligible term, the dominant balance technique typically still involves more than two terms [18–22, 38]. Because the coefficients have the form of a power-law and in OMS only two coefficients are considered simultaneously, the unknowns can be estimated by performing linear algebra operations. The linear algebra approach is not possible when more than two terms are considered simultaneously.

When the two terms balancing each other are the dominant terms, no other term is larger than these. In the asymptotic cases, the non-dominant (secondary) terms tend to zero and the simplified balance tends to the exact solution. In some cases, terms outside the balance tend to neither zero nor infinity in the asymptotic regime, effectively establishing a multiple-term balance. These special cases are the focus of current work, but beyond the scope of this paper. Also, the combination of parameters that fall in between asymptotic regimes require consideration beyond the analysis of asymptotic extremes. Appendix B details the linear algebra aspects of multiple-term balances.

2.2.3 Practical considerations of modified dominant balance

Because the coefficients have the form of a power-law and only two coefficients are considered simultaneously, the unknowns can be estimated by performing linear algebra operations. Calling q the number of unknown characteristic values, then q equations must be considered in each balance.

In OMS, there can be fewer unknown characteristic values than equations. In this case, a subset of the original equations must be chosen to avoid overdetermination. The number

of equations in this subset must match the number of unknown characteristic values q . Self consistent balances must be found for this subset of equations. The remaining equations must be normalized by their largest coefficient, this way self consistency is automatically assured. The normalized remaining equations can be used as a check for the normalization of differential expressions involved in them. When there are more unknown characteristic values than governing equations, a division in subdomains can add new equations to generate a well defined problem. In some cases, such as moving boundary problems, additional equations can be generated by incorporating integral formulations of the governing equations.

For systems involving many equations with many terms, the number of possible two-term balances increases exponentially. An upper bound estimation of the number of balances, which is useful to estimate maximum computational time, is presented in Appendix C.

2.3 Matrix Operations to Estimate the Unknowns

Each of the iterations performed results in a set of normalized equations, where each coefficient in the equation can be obtained by subtracting the row corresponding to the normalizing term from all rows corresponding to terms in that equation. The matrix of normalized coefficients is defined as:

$${}^{(N)} = [N] \left\{ \begin{array}{c} {}^{(K)} \\ {}^{(P)} \\ {}^{(S)} \end{array} \right\} \quad (4)$$

where ${}^{(N)}$ is the column vector of logarithms of normalized coefficients, and $[N]$ is the matrix of normalized coefficients, and ${}^{(K)}$ is the vector of logarithms of the numerical constants, ${}^{(P)}$

the vector of logarithms of the parameters, and (S) the vector of logarithms of the unknown characteristic values.

Appendix D shows that the characteristic values can be estimated using the following matrix operation:

$$(\widehat{S}) = [S](P') \quad (5)$$

where the matrix of scaling factors $[S]$ contains the exponents of the parameters in the estimations of the unknowns.

$$[S] = -[N_o]_S^{-1}[N_o]_{P'} \quad (6)$$

This equation enables the estimation of the characteristic values in a system of equations without solving the actual system; this is still true even if the system includes non-linear differential equations. This expression is novel, and it is at the core of the OMS methodology because it allows computer estimation of characteristic values without manual operations.

2.4 Consistency of Estimations

Checking for self-consistency corresponds to Step 6 in Table 1. Equation 5 yields many different estimates, depending on the terms chosen in the balances. Estimates which result in the secondary terms larger than the assumed dominant terms must be discarded. Thus, for each dominant balance iteration, there are three possible outcomes in OMS: self-consistent, inconsistent, and incompatible. The classification is based on estimations of the neglected terms using the estimates of Equation 5.

To accomplish a classification of consistency, the “matrix of normalized secondary coefficients” $[N_s]$ is defined. In this matrix, each row is a row of matrix $[N]$ that corresponds

to a secondary term. Replacing the unknown characteristic values in $[N_s]$ by their estimates results in

$$(\widehat{N}_s) = [\widehat{N}_s](P') \quad (7)$$

where the notation described in Appendix A indicates:

$$[\widehat{N}_s] = [N_s]_{P'} + [N_s]_S[S] \quad (8)$$

An extension of Equation 8 supplies all coefficients of the normalized equations:

$$[\widehat{N}] = [N]_{P'} + [N]_S[S] \quad (9)$$

Using Equations 7 or 8, a “regime” of a system can be defined as any combination of parameters that result in small secondary terms. The limits of a regime are the combinations of parameters that yield a normalized secondary coefficient equal to 1. Tracing the limits of regimes is essential to create process maps. Of course, the sharp limits obtained are just markers of the gradual transition between regimes, not exact values. The criteria for consistency can then be summarized as:

- All elements of (\widehat{N}_s) are ≤ 0 \Rightarrow self-consistent
- There is an element of (\widehat{N}_s) that is > 0 \Rightarrow inconsistent
- Matrix $[N_o]_{P'}$ is singular \Rightarrow incompatible

2.5 Summary of OMS algorithm

The OMS algorithm is illustrated schematically in Figure 2, and has three main stages. The first stage consists of representing the governing equations in matrix form: the matrix

of coefficients. This stage contains Steps 1, 2, and 3 of Table 1, and requires engineering judgment for the proper normalization of expressions. The second stage involves iterations and matrix operations that solve for the unknowns. This stage contains Steps 4 to 7 of Table 1 and is performed automatically; its outcome is a set of self-consistent scaling laws. Typically, many balances are associated to the same set of scaling laws and are grouped into classes. The third stage involves the assessment of results from the iterations, and it involves a manual check to verify the proper normalization of differential expressions and the presence of special cases of self-consistency or stiff equations.

3 Case study: Thermocapillary flow in welding

The problem considered is the estimation of velocities, pressure, and temperatures due to thermocapillary convection in the weld pool. The formulation used is that of Regime I (no boundary layers) in [13], for which there are known and accepted scaling laws [53–56]. Work on scaling laws in regimes involving boundary layers is also in [13, 39, 55, 56], and most recently in [57].

Figure 3 illustrates the geometry considered, consisting of long channel with its axis perpendicular to the page. The walls of the channel are at temperature T_0 (melting temperature of the metal), and the molten metal receives heat on its free surface from a long, stationary heat source of characteristic half-width \mathcal{L} . There is a large difference between the idealized representation considered here and a real welding problem; however, for many relevant cases, the physical mechanism considered is representative of reality, and the resulting scaling laws are useful in practice. Noteworthy idealizations incurred in the treatment below

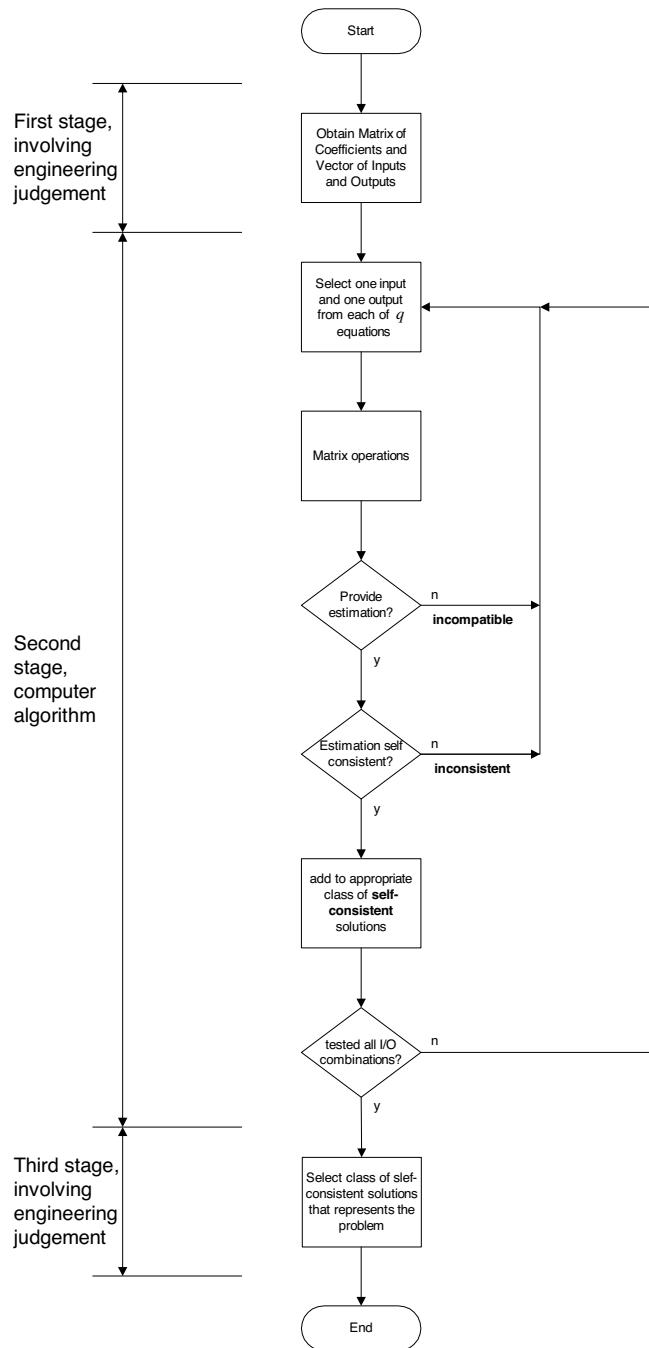


Figure 2: Flowchart of the OMS procedure [1].

are: non-deformable free-surface, heat source stationary with respect to solid boundaries, 2-D rectangular geometry in steady-state, lack of electromagnetic or buoyance body forces in the melt, no gas shear on the surface, no frictional heating, and width of solid boundaries much larger than width of heat source. Also, the fluid is considered laminar, incompressible and with constant thermophysical properties.

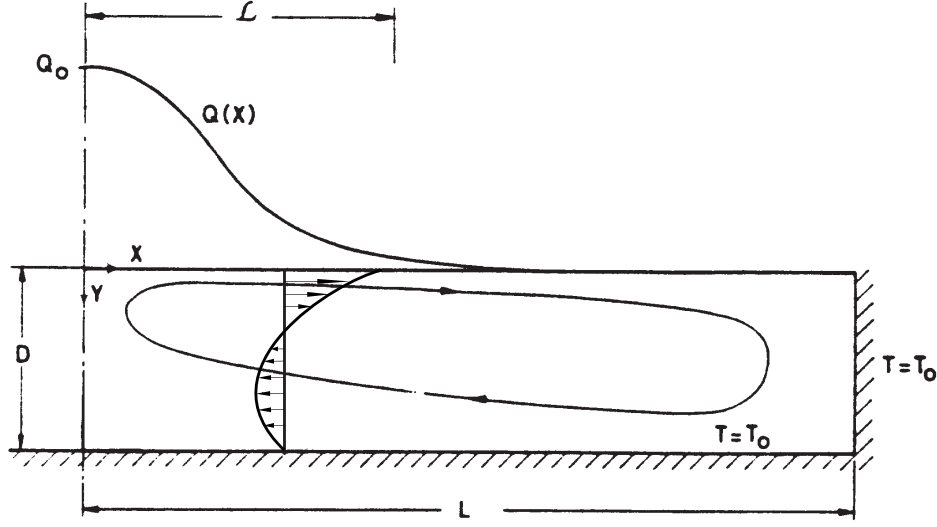


Figure 3: System coordinates and problem configuration for thermocapillary flows (modified from [13]). Only half the enclosure is shown

Based on the above considerations, the mathematical formulation of the problem involves the equation of mass conservation, two Navier-Stokes equations, and conservation of energy:

$$\frac{\partial u}{\partial x} + \frac{\partial v}{\partial y} = 0 \quad (10)$$

$$u \frac{\partial u}{\partial x} + v \frac{\partial u}{\partial y} = -\frac{1}{\rho} \frac{\partial p}{\partial x} + \nu \left(\frac{\partial^2 u}{\partial x^2} + \frac{\partial^2 u}{\partial y^2} \right) \quad (11)$$

$$u \frac{\partial v}{\partial x} + v \frac{\partial v}{\partial y} = -\frac{1}{\rho} \frac{\partial p}{\partial y} + \nu \left(\frac{\partial^2 v}{\partial x^2} + \frac{\partial^2 v}{\partial y^2} \right) \quad (12)$$

$$u \frac{\partial T}{\partial x} + v \frac{\partial T}{\partial y} = \alpha \left(\frac{\partial^2 T}{\partial x^2} + \frac{\partial^2 T}{\partial y^2} \right) \quad (13)$$

Non slip and symmetry boundary conditions apply as indicated in Figure 3. The surface pressure far from the heat source is atmospheric. The boundary conditions are what makes this problem interesting, and involve the Marangoni boundary condition as well as a heat input condition, both on the free surface:

$$\rho\nu\frac{\partial u}{\partial y} = \sigma_T\frac{\partial T}{\partial x} \quad (14)$$

$$k\frac{\partial T}{\partial y} = -Q(x) \quad (15)$$

The independent variables are $\{X\} = \{x, y\}$ (shown in Figure 3); the dependent variables are $\{U\} = \{u(x, y), v(x, y), p(x, y), T(x, y)\}$, representing the x and y components of the velocity field, the pressure field, and the temperature field; and the parameters are $\{P\} = \{\mathcal{L}, \rho, \alpha, k, Q_0, \sigma_T, \nu, D\}$ representing a characteristic half width of the heat source, the melt density, the melt thermal diffusivity, the melt thermal conductivity, the maximum intensity of the heat source, the variation in surface tension with temperature, the kinematic viscosity, and the depth of the melt. These parameters represent an autogenous weld on 304 stainless steel ($\rho=6907 \text{ kg/m}^3$, $\nu=8.32 \cdot 10^{-7} \text{ m}^2/\text{s}$, $\alpha=3.3 \cdot 10^{-6} \text{ m}^2/\text{s}$, $k=18 \text{ Wm}^{-1}\text{K}^{-1}$ [39]) with 40 ppm of S ($\sigma_T=1.5 \cdot 10^{-9} \text{ Nm}^{-1}\text{K}^{-1}$ [58]) using a defocused laser or a GTAW torch with an argon arc of 70 A and 2 mm length ($\mathcal{L}=1.2 \text{ mm}$, $Q_0=4 \cdot 10^7 \text{ W/m}^{-2}$ [59]) and depth $D=0.6 \text{ mm}$ (typical value). The value of 40 ppm S was chosen such that the flow in the weld pool would be dominated by viscous forces.

3.1 Construction of the Matrix of Coefficients

Using the normalization scheme described in [2], the independent variables are normalized as $x^* = x/\mathcal{L}$ and $y^* = y/D$, and the normalized counterpart of equations 10-13 is:

$$\left(\frac{\partial u}{\partial x}\right)_c \left(\frac{\partial u}{\partial x}\right)^* + \left(\frac{\partial v}{\partial y}\right)_c \left(\frac{\partial v}{\partial y}\right)^* = 0 \quad (16)$$

$$\begin{aligned} \left(u\frac{\partial u}{\partial x}\right)_c \left(u\frac{\partial u}{\partial x}\right)^* + \left(v\frac{\partial u}{\partial y}\right)_c \left(v\frac{\partial u}{\partial y}\right)^* &= -\frac{1}{\rho} \left(\frac{\partial p}{\partial x}\right)_c \left(\frac{\partial p}{\partial x}\right)^* + \\ &+ \nu \left(\frac{\partial^2 u}{\partial x^2}\right)_c \left(\frac{\partial^2 u}{\partial x^2}\right)^* + \nu \left(\frac{\partial^2 u}{\partial y^2}\right)_c \left(\frac{\partial^2 u}{\partial y^2}\right)^* \end{aligned} \quad (17)$$

$$\begin{aligned} \left(u\frac{\partial v}{\partial x}\right)_c \left(u\frac{\partial v}{\partial x}\right)^* + \left(v\frac{\partial v}{\partial y}\right)_c \left(v\frac{\partial v}{\partial y}\right)^* &= -\frac{1}{\rho} \left(\frac{\partial p}{\partial y}\right)_c \left(\frac{\partial p}{\partial y}\right)^* + \\ &+ \nu \left(\frac{\partial^2 v}{\partial x^2}\right)_c \left(\frac{\partial^2 v}{\partial x^2}\right)^* + \nu \left(\frac{\partial^2 v}{\partial y^2}\right)_c \left(\frac{\partial^2 v}{\partial y^2}\right)^* \end{aligned} \quad (18)$$

$$\begin{aligned} \left(u\frac{\partial T}{\partial x}\right)_c \left(u\frac{\partial T}{\partial x}\right)^* + \left(v\frac{\partial T}{\partial y}\right)_c \left(v\frac{\partial T}{\partial y}\right)^* &= \\ &= \alpha \left(\frac{\partial^2 T}{\partial x^2}\right)_c \left(\frac{\partial^2 T}{\partial x^2}\right)^* + \alpha \left(\frac{\partial^2 T}{\partial y^2}\right)_c \left(\frac{\partial^2 T}{\partial y^2}\right)^* \end{aligned} \quad (19)$$

with normalized boundary conditions:

$$\rho\nu \left(\frac{\partial u}{\partial y}\right)_c \left(\frac{\partial u}{\partial y}\right)^* = \sigma_T \left(\frac{\partial T}{\partial x}\right)_c \left(\frac{\partial T}{\partial x}\right)^* \quad (20)$$

$$k \left(\frac{\partial T}{\partial y}\right)_c \left(\frac{\partial T}{\partial y}\right)^* = -Q_0 Q^*(x^*) \quad (21)$$

Table 2 lists the characteristic values of differential expressions calculated using the traditional normalization approach described in [2]. These characteristic values were assigned assuming there are no boundary layers; at this stage, this is only a supposition, but it will be verified later in this paper. Based on equations 16-21 and Table 2 the corresponding matrix of coefficients $[C]$ is shown in Equation 22.

Table 2: Estimated characteristic values for equations 16-21

Characteristic value	Estimation
$(\partial u / \partial x)_c$	u_c / \mathcal{L}
$(\partial u / \partial y)_c$	u_c / D
$(\partial v / \partial y)_c$	v_c / D
$(\partial p / \partial x)_c$	p_c / \mathcal{L}
$(\partial p / \partial y)_c$	p_c / D
$(u \partial u / \partial x)_c$	u_c^2 / \mathcal{L}
$(v \partial u / \partial y)_c$	$v_c u_c / D$
$(u \partial v / \partial x)_c$	$u_c v_c / \mathcal{L}$
$(v \partial v / \partial y)_c$	v_c^2 / D
$(u \partial T / \partial x)_c$	$u_c T_c / \mathcal{L}$
$(v \partial T / \partial y)_c$	$v_c T_c / D$
$(\partial^2 u / \partial x^2)_c$	u_c / \mathcal{L}^2
$(\partial^2 u / \partial y^2)_c$	u_c / D^2
$(\partial^2 v / \partial x^2)_c$	v_c / \mathcal{L}^2
$(\partial^2 v / \partial y^2)_c$	v_c / D^2
$(\partial T / \partial x)_c$	T_c / \mathcal{L}
$(\partial T / \partial y)_c$	T_c / D
$(\partial^2 T / \partial x^2)_c$	T_c / \mathcal{L}^2
$(\partial^2 T / \partial y^2)_c$	T_c / D^2

$$[C] = \begin{bmatrix}
\mathcal{L} & D & \rho & \nu & \alpha & k & \sigma_T & Q_0 & u_c & v_c & p_c & T_c \\
-1 & & & & & & & & 1 & & & \\
& -1 & & & & & & & & 1 & & \\
-1 & & & & & & & & 2 & & & \\
& -1 & & & & & & & 1 & 1 & & \\
-1 & & -1 & & & & & & & & 1 & \\
-2 & & & 1 & & & & & 1 & & & \\
& -2 & & 1 & & & & & 1 & & & \\
-1 & & & & & & & & 1 & 1 & & \\
& -1 & & & & & & & & 2 & & \\
-1 & -1 & & & & & & & & & 1 & \\
-2 & & & 1 & & & & & 1 & & & \\
& -2 & & 1 & & & & & 1 & & & \\
-1 & & & & & & & & 1 & & 1 & \\
& -1 & & & & & & & & 1 & & 1 \\
-2 & & & & 1 & & & & & & & 1 \\
& -2 & & & 1 & & & & & & & 1 \\
& -1 & 1 & 1 & & & & & 1 & & & \\
-1 & & & & & & 1 & & & & & 1 \\
& -1 & & & & 1 & & & & & & 1 \\
& & & & & & & 1 & & & &
\end{bmatrix}
\begin{matrix}
\text{Eq. 16} \\
\text{Eq. 17} \\
\text{Eq. 18} \quad (22) \\
\text{Eq. 19} \\
\text{Eq. 20} \\
\text{Eq. 21}
\end{matrix}$$

3.2 Iterations based on matrix operations

The construction of the matrix of coefficients completes the first stage of OMS. The matrix operations of this section constitute the second stage, performed automatically by a computer. For the matrix of coefficients of Equation 22, the OMS algorithm tried 2,486 combinations of four pairs of balancing terms in 0.76 s in a MacBook with a 2.4 GHz processor. This exhaustive analysis identified 1,897 incompatible balances, 544 inconsistent balances and 45 self-consistent balances. The 45 self-consistent balances correspond to 14 classes, with each class made of all balances that result in the same estimation. Of the 45 classes of self-consistent balances, only 2 are consistent with mass conservation (Equation 10) and the boundary conditions (equations 14 and 15). The matrix of normalized coefficients for one of these two classes is shown in Equation 23. This matrix has six rows with only zeros (not shown) because these rows correspond to terms used to normalize the equations.

$$[N] = \begin{array}{c}
 \begin{array}{cccccccc|cccc}
 \mathcal{L} & D & \rho & \nu & \alpha & k & \sigma_T & Q_0 & u_c & v_c & p_c & T_c \\
 \hline
 -1 & -1 & & & & & & & 1 & -1 & & \\
 \hline
 -1 & 2 & & -1 & & & & & 1 & & & \\
 & 1 & & -1 & & & & & & 1 & & \\
 -1 & 2 & -1 & -1 & & & & & -1 & & 1 & \\
 -2 & 2 & & & & & & & & & & \\
 \hline
 -1 & 1 & 1 & & & & & & 1 & 1 & -1 & \\
 & & 1 & & & & & & & 2 & -1 & \\
 -2 & 1 & 1 & 1 & & & & & & 1 & -1 & \\
 & -1 & 1 & 1 & & & & & & 1 & -1 & \\
 \hline
 -1 & 2 & & & -1 & & & & 1 & & & \\
 & 1 & & & -1 & & & & & 1 & & \\
 -2 & 2 & & & & & & & & & & \\
 \hline
 1 & -1 & 1 & 1 & & & -1 & & 1 & & & -1 \\
 \hline
 & -1 & & & & 1 & & -1 & & & & 1
 \end{array} \\
 \begin{array}{l}
 \text{Eq. 16} \\
 \\
 \\
 \text{Eq. 17} \\
 \\
 \\
 \text{Eq. 18} \quad (23) \\
 \\
 \\
 \text{Eq. 19} \\
 \\
 \text{Eq. 20} \\
 \\
 \text{Eq. 21}
 \end{array}
 \end{array}$$

The only difference between the two chosen classes is in the scaling law for \widehat{p}_c , and the determination of the valid class requires engineering judgement in the Stage 3 in Figure 2. The criterion of class selection will be explained later. The selected matrix of scaling factors is:

$$[S] = \begin{array}{cccccccc} \mathcal{L} & D & \rho & \nu & \alpha & k & \sigma_T & Q_0 \\ \left[\begin{array}{cccccccc} -1 & 2 & -1 & -1 & & -1 & 1 & 1 \\ -2 & 3 & -1 & -1 & & -1 & 1 & 1 \\ & & & & & -1 & 1 & 1 \\ & 1 & & & & -1 & & 1 \end{array} \right] & \begin{array}{l} \widehat{u}_c \\ \widehat{v}_c \\ \widehat{p}_c \\ \widehat{T}_c \end{array} \end{array} \quad (24)$$

yielding the following estimates:

$$\widehat{u}_c = \frac{D^2 \sigma_T Q_0}{\mathcal{L} \rho \nu k} = 0.17 \text{ mm/s} \quad (25)$$

$$\widehat{v}_c = \frac{D^3 \sigma_T Q_0}{\mathcal{L}^2 \rho \nu k} = 0.09 \text{ mm/s} \quad (26)$$

$$\widehat{p}_c = \sigma_T Q_0 / k = 0.0033 \text{ Pa} \quad (27)$$

$$\widehat{T}_c = D Q_0 / k = 1,333 \text{ K} \quad (28)$$

Equations 25 to 28 are exactly the same as those obtained manually in [13]. The velocities obtained are smaller than usual. This is because the thermocapillary coefficient chosen (σ_T) is very small. Such small value is possible, but unstable, because small variations in surface active elements can radically alter the results.

This thermocapillary flow problem was scaled manually in [13, 55, 56]; in these cases, manual scaling was possible only because \widehat{u}_c , \widehat{v}_c , and \widehat{T}_c can be obtained by considering equations 10, 14, and 15 alone, and since they involve only two terms each, only one balance is possible. After the determination, \widehat{u}_c , \widehat{v}_c , and \widehat{T}_c , the exhaustive manual determination

of \widehat{p}_c still involves 26 iterations. Only Rivas and Ostrach [13] describe considerations of pressure, arriving to the same result as in this section; however, they do not discuss the other self-consistent balance and offer no explanation for their choice.

The set of governing equations based on normalized variables can be written using the linear algebra operations from OMS and the traditional approach to characteristic values, where $(\partial u / \partial x)^* = \partial u^* / \partial x^*$ and so forth, with normalized variables $x^* = \mathcal{L} / x$, $y^* = y / D$, $u^* = u / \widehat{u}_c$, $v^* = v / \widehat{v}_c$, $p^* = p / \widehat{p}_c$, $T^* = (T - T_0) / \widehat{T}_c$. The balance selected yields the matrix of normalized coefficients $[\widehat{N}]$ of Equation 29, where the zero elements are omitted. Because the dominant input and output terms have a coefficient of 1 when normalized, their corresponding rows in $[\widehat{N}]$ have only zeros and appear as empty lines. Because equations 10, 14, and 15 are used on the selected balance and they only have only two terms each, they appear as completely empty rows in Equation 29

$$\begin{aligned}
& \begin{matrix} \mathcal{L} & D & \rho & \nu & \alpha & k & \sigma_T & Q_0 \\ \left[\begin{array}{cccccccc} & & & & & & & \\ \hline -2 & 4 & -1 & -2 & & -1 & 1 & 1 \\ -2 & 4 & -1 & -2 & & -1 & 1 & 1 \\ \\ -2 & 2 & & 1 & & & & \\ \hline -4 & 6 & -1 & -2 & & -1 & 1 & 1 \\ -4 & 6 & -1 & -2 & & -1 & 1 & 1 \\ \\ -4 & 4 & & & & & & \\ -2 & 2 & & & & & & \\ \hline -2 & 4 & -1 & -1 & -1 & -1 & 1 & 1 \\ -2 & 4 & -1 & -1 & -1 & -1 & 1 & 1 \\ -2 & 2 & & & & & & \\ \hline \\ \hline \end{array} \right] \end{matrix} & \begin{matrix} \text{Eq. 16} \\ \\ \\ \text{Eq. 17} \\ \\ \\ \text{Eq. 18} \\ \\ \text{Eq. 19} \\ \\ \text{Eq. 20} \\ \\ \text{Eq. 21} \end{matrix} \\
[\widehat{N}] = & \quad \quad \quad (29)
\end{aligned}$$

Using matrix $[\widehat{N}]$, the original set of equations 10 to 15 can be expressed in dimensionless form as:

$$\frac{\partial u^*}{\partial x^*} + \frac{\partial v^*}{\partial y^*} = 0 \quad (30)$$

$$\left(\frac{D^4 \sigma_T Q_0}{\mathcal{L}^2 \rho \nu^2 k}\right) u^* \frac{\partial u^*}{\partial x^*} + \left(\frac{D^4 \sigma_T Q_0}{\mathcal{L}^2 \rho \nu^2 k}\right) v^* \frac{\partial u^*}{\partial y^*} = \frac{\partial p^*}{\partial x^*} + \left(\frac{D \nu}{\mathcal{L}^2}\right) \frac{\partial^2 u^*}{\partial x^{*2}} + \frac{\partial^2 u^*}{\partial y^{*2}} \quad (31)$$

$$\left(\frac{D^6 \sigma_T Q_0}{\mathcal{L}^4 \rho \nu^2 k}\right) u^* \frac{\partial v^*}{\partial x^*} + \left(\frac{D^6 \sigma_T Q_0}{\mathcal{L}^4 \rho \nu^2 k}\right) v^* \frac{\partial v^*}{\partial y^*} = \frac{\partial p^*}{\partial y^*} + \left(\frac{D^4}{\mathcal{L}^4}\right) \frac{\partial^2 v^*}{\partial x^{*2}} + \left(\frac{D^2}{\mathcal{L}^2}\right) \frac{\partial^2 v^*}{\partial y^{*2}} \quad (32)$$

$$\left(\frac{D^4 \sigma_T Q_0}{\mathcal{L}^2 \rho \nu \alpha k}\right) u^* \frac{\partial T^*}{\partial x^*} + \left(\frac{D^4 \sigma_T Q_0}{\mathcal{L}^2 \rho \nu \alpha k}\right) v^* \frac{\partial T^*}{\partial y^*} = \left(\frac{D^2}{\mathcal{L}^2}\right) \frac{\partial^2 T^*}{\partial x^{*2}} + \frac{\partial^2 T^*}{\partial y^{*2}} \quad (33)$$

including normalized boundary conditions:

$$\frac{\partial u^*}{\partial y^*} = \frac{\partial T^*}{\partial x^*} \quad (34)$$

$$\frac{\partial T^*}{\partial y^*} = Q^*(x^*) \quad (35)$$

In the asymptotic extreme of negligible convection, negligible inertial forces, and very shallow melt, the coefficients in parentheses tend to zero with no singularity of any type in the limit. Matrix $[\widehat{N}]$ shows that in Equation 18 (Navier-Stokes in y) has only its third term, representing the pressure gradient between the free surface and the bottom, with a coefficient of unity. Similarly, only the fourth term of Equation 19, representing the temperature gradient between the free surface and the bottom in the energy equation, has a coefficient of 1. This indicates that in the asymptotic extreme $\partial p^*/\partial y^* \rightarrow 0$ and $\partial^2 T^*/\partial y^{*2} \rightarrow 0$, and it can be interpreted as “pressure in the fluid is imposed from the surface” and “temperature varies linearly across the depth of the weld pool.” The interpretation of pressure behavior is similar to that in Prantl’s asymptotic analysis of the boundary layer, while the interpretation of temperature variation is consistent with a one-dimensional conduction-dominated system.

3.3 Final Choice of Self-Consistent Balance

It was mentioned above that the OMS algorithm yielded two self-consistent balances, of which the chosen one was described above. This section addresses the reasoning behind this choice. The discarded balance results in equations 30, 33, 34, 35, and a pressure estimation of $\hat{p}_c = (D/\mathcal{L})^2 \sigma_T Q_0 / k$. However, the dimensionless Navier-Stokes equations are different in this balance:

$$\left(\frac{D^4 \sigma_T Q_0}{\mathcal{L}^2 \rho \nu^2 k} \right) u^* \frac{\partial u^*}{\partial x^*} + \left(\frac{D^4 \sigma_T Q_0}{\mathcal{L}^2 \rho \nu^2 k} \right) v^* \frac{\partial u^*}{\partial y^*} = \left(\frac{D^2}{\mathcal{L}^2} \right) \frac{\partial p^*}{\partial x^*} + \left(\frac{D\nu}{\mathcal{L}^2} \right) \frac{\partial^2 u^*}{\partial x^{*2}} + \frac{\partial^2 u^*}{\partial y^{*2}} \quad (36)$$

$$\left(\frac{D^4 \sigma_T Q_0}{\mathcal{L}^2 \rho \nu^2 k} \right) u^* \frac{\partial v^*}{\partial x^*} + \left(\frac{D^4 \sigma_T Q_0}{\mathcal{L}^2 \rho \nu^2 k} \right) v^* \frac{\partial v^*}{\partial y^*} = \frac{\partial p^*}{\partial y^*} + \left(\frac{D^2}{\mathcal{L}^2} \right) \frac{\partial^2 v^*}{\partial x^{*2}} + \frac{\partial^2 v^*}{\partial y^{*2}} \quad (37)$$

Equation 36 has a coefficient of 1 only for the term representing the curvature of the profile of horizontal component of the velocity. This means that in the asymptotic extreme the horizontal velocity varies linearly across the depth of the weld pool, but this is impossible for recirculating flows with a no-slip condition at the bottom, as shown in Figure 3.

3.4 Limit of validity of estimates

The scaling estimates for \hat{u}_c , \hat{v}_c , \hat{p}_c , and \hat{T}_c are the result of considering only the dominant forces present and assuming the secondary forces are zero. In this example the dominant forces considered are Marangoni driven flows balanced by viscous forces, and a surface heat source balanced by heat conduction; the neglected phenomena are inertial forces and convective heat transfer. Because the obtained scaling expressions are the same as long as the approximations made are valid, it is crucial to determine their range of validity to trust them enough to use in practice.

The asymptotic approximations are invalid when the balances become inconsistent, i.e., when the dimensionless groups associated with the secondary coefficients are greater than 1; this way, the limits of validity of equations 25 to 28 are given by:

$$\left(\frac{D^4 \sigma_T Q_0}{\mathcal{L}^2 \rho \nu^2 k} \right) \leq 1 \quad (38)$$

$$\left(\frac{D \nu}{\mathcal{L}^2} \right) \leq 1 \quad (39)$$

$$\left(\frac{D^6 \sigma_T Q_0}{\mathcal{L}^4 \rho \nu^2 k} \right) \leq 1 \quad (40)$$

$$\left(\frac{D^4}{\mathcal{L}^4} \right) \leq 1 \quad (41)$$

$$\left(\frac{D^2}{\mathcal{L}^2} \right) \leq 1 \quad (42)$$

$$\left(\frac{D^4 \sigma_T Q_0}{\mathcal{L}^2 \rho \nu \alpha k} \right) \leq 1 \quad (43)$$

It is obvious that not all these dimensionless groups are independent among themselves, and a base set can be determined manually. Dimensional analysis considerations in OMS determine the number of dimensionless groups involved, and sets the stage for further operations.

3.5 Dimensional Analysis considerations

The number of independent dimensionless groups in system (m) is very easy to determine with OMS: it is the number of independent rows in matrix $[\widehat{N}]$; therefore:

$$m = \text{rank}[\widehat{N}] \quad (44)$$

which for this example yields $m = 3$, meaning that there only three independent dimensionless groups can exist simultaneously; this can be confirmed to be the case by manually

manipulating equations 38-43. The OMS result is better than what would have been obtained by using Buckingham's theorem [44], which establishes that for the 8 parameters of this problem with the 4 reference units involved (m, kg, s, K), there should be four (not three) dimensionless groups. The reason for the discrepancy is that in the set of governing equations, mechanical and thermal energy are never converted into each other, resulting in the possibility of using two independent reference units for energy [39]. The consideration of an additional reference unit for thermal energy would make Buckingham's theorem yield the correct number of dimensionless groups.

The three reference dimensionless groups chosen must be based solely on the problem parameters, and their choice is arbitrary with the only constriction that they must be mutually independent. Following [13], the following set is chosen:

$$\text{Re}_\sigma = \hat{u}_c \mathcal{L} / \nu = \frac{D^2 \sigma_T Q_0}{\rho \nu^2 k} \quad (45)$$

$$\text{Pr} = \nu / \alpha \quad (46)$$

$$A = D / \mathcal{L} \quad (47)$$

where Re_σ is the Reynolds number obtained using a velocity estimate, Pr is the Prandtl number, and A is the aspect ratio. It is interesting to highlight that the Marangoni number is not necessary to completely describe the system with the current choice of reference dimensionless groups. Of course, the Marangoni number could be constructed by combination of the chosen groups as $\text{Ma} = \text{Re}_\sigma \text{Pr}$.

The range of validity given by equations 38-43 can then be expressed in terms of the

reference dimensionless groups as:

$$A \leq 1 \tag{48}$$

$$\text{Re}_\sigma A^2 \leq 1 \tag{49}$$

$$\text{Re}_\sigma \text{Pr} A^2 \leq 1 \tag{50}$$

The above expressions can be obtained manually from equations 38-43, or from linear algebra operations within the OMS framework. For the stainless steel welding example, the corresponding values are: $\text{Re}_\sigma=0.25$, $\text{Pr}=0.25$, and $A=0.5$.

3.6 Process maps

Figure 4 displays the graphic representation of equations 48-50 for shallow enclosures ($A \leq 1$). The dot labelled “SS 304” corresponds to the stainless steel welding example considered. The dashed lines delimiting the shaded region represent the “envelope” of the regime considered; dashed lines are used as a reminder that the regime limits are not sharp, and as the lines are approached, the secondary terms approach the order of magnitude of the dominant terms, and the estimates can diverge from the actual values. The representation of range of validity of one or more regimes in Figure 4 constitutes a “process map.”

Process maps are of great practical use. Any system described by governing equations 10-15 can be located on the map using only the problem parameters, which are known *a priori*. Once a particular system has been located on the map, scaling estimates and correction factors can be determined using only the problem parameters. The use of correction factors based on dimensionless groups that capture secondary effects is addressed in [60–62].

Other regimes are possible in this problem, and would be graphically represented in

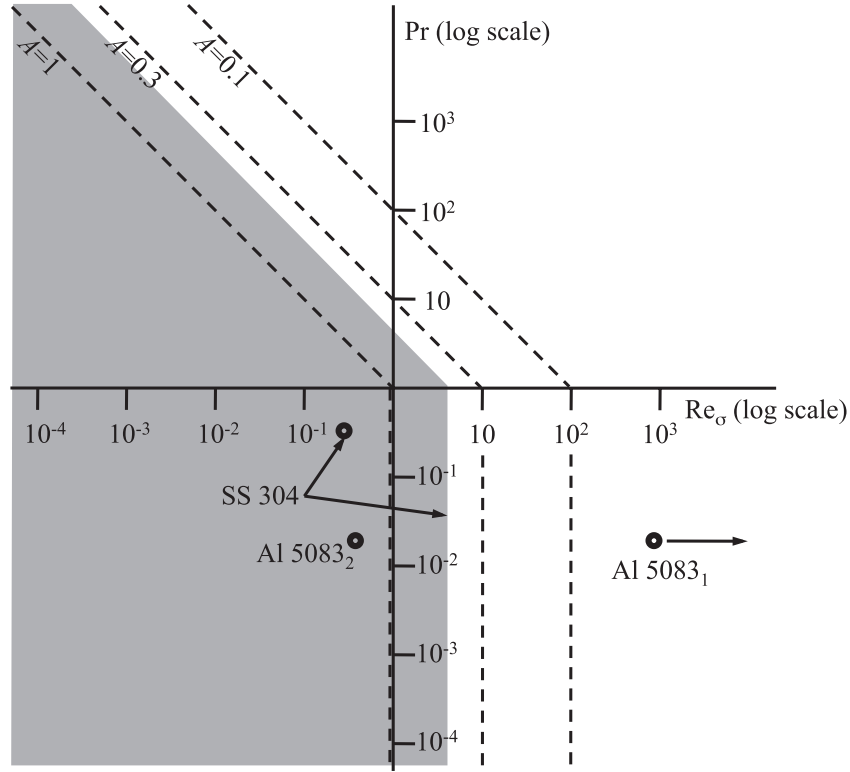


Figure 4: Process map for thermocapillary flows. The dashed lines indicate the the range of self-consistency of scaling estimates from equations 25 to 28 for different values of aspect ratio A . The shaded area and the dot labelled “SS 304” correspond to the values used in the stainless steel example ($Re_\sigma=0.25$, $Pr=0.25$, $A=0.5$). The dot labelled “Al 5083₂” corresponds to the self-consistent aluminum example ($Re_\sigma=0.36$, $Pr=0.018$, $A=0.9$), and the point “Al 5083₁ the the inconsistent aluminum example($Re_\sigma=1.3 \cdot 10^6$, $Pr=0.018$, $A=0.9$).

Figure 4 by points that fall outside the shaded area. For low Prandtl numbers, these regimes were reviewed in [13, 39]. Each regime has a different scaling involving the presence or absence of boundary layers and the dominant heat and momentum transport mechanism: conduction vs. convection, and viscous vs. inertial. For the problem considered, the set of dimensionless governing equations 30-35 involves two-term balances with no singularity, confirming the original hypothesis of absence of boundary layers. It is interesting to highlight that for shallow enclosures ($A \ll 1$, values of Re_σ and Pr can be relatively large and the system still be dominated by conduction and viscosity.

For very shallow enclosures the flow pattern might result in Bénard-Marangoni convective cells instead of a single recirculating loop; in this case the estimated characteristic values of Table 2 should be revisited. Convective cells will happen when the Marangoni number exceeds a value of 80 [63]. Equation 50 indicates that cell convection should not be a problem for the regime studied for aspect ratio $A > 0.11$, which covers the typical values of welding.

3.7 Example of application of process map

Consider an autogenous weld on aluminum 5083 made by a Nd:YAG fiber laser. The beam is set to a power $W = 4$ kW, a FWHM (full width half maximum) spot size of 1 mm, and a beam velocity of 10 mm/s. The beam efficiency is $\eta = 15\%$. The penetration configuration of the weld pool is in “conduction mode” with a penetration of $D = 0.45$ mm. The label “conduction mode” indicates the absence of a keyhole, and it is used by welders and researchers even if the dominant heat transfer mechanism is convection in the molten metal. The thermophysical properties of molten aluminum 5083 at 800 °C are $\rho = 2309$ kg/m³, $\nu = 4.33 \cdot 10^{-7}$

m^2/s , $\alpha=2.4 \cdot 10^{-5} \text{ m}^2/\text{s}$, and $k=68 \text{ Wm}^{-1}\text{K}^{-1}$ [64]. Two surface tension temperature coefficients will be considered: $\sigma_{T_1}=3.5 \cdot 10^{-4} \text{ Nm}^{-1}\text{K}^{-1}$ as used in [65], and the artificial value $\sigma_{T_2}=10^{-10} \text{ Nm}^{-1}\text{K}^{-1}$.

The question to answer is: *What are the representative surface velocity and maximum temperature in the weld?* This question is very difficult to answer without the help of a process map and order of magnitude estimates. Fortunately, the thermocapillary flow model discussed above is a reasonable idealization useful to answer this question.

The first step is to calculate the values of the parameters for the model. The length $\mathcal{L}=0.5$ mm is assigned as half the FWHM. Assuming the beam has a typical gaussian distribution, the maximum heat intensity is $Q_0 = \eta W / (2\pi\sigma_b^2)$, where σ_b is the standard deviation of the beam heat distribution, related to the FWHM by $\sigma_b = \text{FWHM} / (2\sqrt{2\ln 2}) \approx \text{FWHM} / 2.36$ resulting in $Q_0=5.3 \cdot 10^8 \text{ W/m}^{-2}$.

The parameters calculated for this example yield two different sets of dimensionless groups depending on the value considered for the surface tension temperature coefficient. For σ_{T_1} , the corresponding coordinates in the process map are $\text{Re}=1.3 \cdot 10^6$, $\text{Pr}=1.8 \cdot 10^{-2}$, $A=0.9$, indicated as Al 5083₁ in Figure 4. For σ_{T_2} , the coordinates are $\text{Re}=0.36$, $\text{Pr}=1.8 \cdot 10^{-2}$, $A=0.9$, indicated as Al 5083₂. Using these groups as coordinates in the process map of Figure 4, point Al 5083₁ falls outside the self-consistent range for the regime studied, while point Al 5083₂ falls in the self-consistent region with known scaling estimates.

For point Al5083₂, the original questions about characteristic surface velocity and temperature are answered using 25 and 28, obtaining $u_c=3.2 \cdot 10^{-4} \text{ m/s}$, and $T_c=3500 \text{ K}$. To obtain the actual maximum temperature, the melting temperature must be considered, which in this case can be considered as $650 \text{ }^\circ\text{C}$, yielding a maximum temperature of $4150 \text{ }^\circ\text{C}$. This

temperature is above the boiling point of aluminum (2519 °C), indicating that the heat input for the system should be decreased accounting for heat losses due to evaporation. In practice, it is generally agreed that the surface of the weld pool has temperatures approaching boiling.

If reliable experimental or numerical results were available, they would seldom be exactly the same as predicted by Equations 25 to 28. Assuming the main sources of discrepancy are the neglect of inertial and convective phenomena, as well as the consideration of finite aspect ratio, the estimates could be corrected to a high degree of accuracy while keeping the generality and simplicity. The correction can be performed using calibration functions based on Re_σ , Pr , and A , as described in [60].

4 Discussion

The scaling laws obtained are exactly the same as the known existing scaling, supporting the validity of the OMS procedure. OMS also allowed for an effortless exhaustive search of all possible balances, and resulted in awareness followed by rigorous and nuanced discussion of the choice of scaling laws when more than one was possible. The existence of multiple self-consistent balances was not discussed in any of the previous literature, and possibly, there was no awareness of it.

OMS could go further than reproducing the manual results already known as shown above. Equations 10 to 15 are an incomplete description of a typical welding problem, since they do not incorporate very important body forces such as the magnetohydrodynamic effect of imposing an electrical current through a conducting fluid. Incorporating such effects would have made the problem intractable with a manual approach. In contrast, the OMS

procedure and matrix operations presented here could deal with more complex equations, tackling the problem computationally with little additional effort for the researcher. The application of OMS to a more complete description of welding is presented in [66,67], where phenomena considered include viscous and inertial forces, Marangoni boundary condition, electromagnetic, buoyancy, and hydrostatic forces, and gas shear at the free surface.

The estimates have two sources of error: the estimation of characteristic values of differential expressions, and the neglecting of secondary terms in the formulation of balances. Estimates that capture the correct asymptotic behavior but differ from measurements by a constant factor can be improved with a single experiment or numerical simulation. The complete independent set of dimensionless groups: Re_σ , Pr , and A can be used to improve the estimates for near-asymptotic cases through regressions based on comparisons with experiments or simulations [68]. The simplified system of governing equations 30-35, is also desirable as a starting point for perturbation analysis.

5 Conclusions

The OMS algorithm has been implemented in prototype form in Matlab and applied to the analysis of thermocapillary driven flows, automatically reproducing the widely accepted solutions for maximum velocity and maximum temperature manually obtained by others in the past. The code, together with insight gained by the framework of analysis, also yielded an estimate for pressure that had seldom been presented, and never discussed.

The OMS algorithm identified a set of three independent dimensionless groups that completely characterizes any thermocapillary flow problem that falls in the formulation used

(Re_σ , Pr , A). These dimensionless groups can be the variables of a formal calibration by comparisons to experiments and numerical models. These dimensionless groups can also become the small parameters in perturbation analysis.

The formal creation of process maps based on the complete set of independent dimensionless groups is described in detail, and a case study is worked out as a demonstration.

A detailed literature search was performed to put the mathematical foundations of OMS in the context of similar work in engineering, physics, applied mathematics, and artificial intelligence. The OMS formulation is unique in its use of the "matrix of coefficients" [C], and in the use of two-term balances. No other formulation of scaling analysis has the capability of determining by itself a self-consistent normalization scheme.

A complete derivation of the key equation for the estimation of unknowns (Equation 6) is included. This derivation had never been presented complete before.

Overall, the thermocapillary flow problem shows that the OMS code can tackle the complexity of welding in a formal way with a minimum of manual involvement, and it is reasonable to expect its successful application to problems of constantly increasing complexity.

6 Acknowledgements

This work was partially supported by NSERC Discovery Grant #G121211200 "Innovation in Materials Processing Using Scaling Principles." Valuable discussions and feedback from S. Gajapathi and K. Tello are gratefully acknowledged.

References

- [1] Mendez, P. F. and Eagar, T. W., 2012, “Order of magnitude scaling: A systematic approach to approximation and asymptotic scaling of equations in engineering,” *Journal of Applied Mechanics*, **in print**.
- [2] Mendez, P. F., —2010—, “Characteristic values in the scaling of differential equations in engineering,” *Journal of Applied Mechanics*, **77**(6), p. 061017 (12 pages).
- [3] Krantz, W. B., —2007—, *Scaling analysis in modeling transport and reaction processes : a systematic approach to model building and the art of approximation*, John Wiley & Sons, Hoboken, N.J.
- [4] Sides, P. J., —2002—, “Scaling of differential equations. ”analysis of the fourth kind”,” *Chemical Engineering Education*, **36**(3), pp. 232–235.
- [5] Deen, W. M., —1998—, *Analysis of transport phenomena*, Oxford University Press, New York.
- [6] Astarita, G., —1997—, “Dimensional analysis, scaling, and orders of magnitude,” *Chemical Engineering Science*, **52**(24), pp. 4681–4698.
- [7] Ruckenstein, E., —1987—, “Analysis of transport phenomena using scaling and physical models,” *Advances in Chemical Engineering*, **13**, pp. 11–112.
- [8] Denn, M. M., —1980—, *Process Fluid Mechanics*, Prentice-Hall International Series in the Physical and Chemical Engineering Series, Prentice-Hall, Englewood Cliffs, NJ, first ed.

- [9] Aris, R., —1976—, “How to get the most out of an equation without really trying,” *Chemical Engineering Education*, **10**(3), pp. 114–124.
- [10] Bejan, A., —2004—, *Convection heat transfer*, Wiley, Hoboken, N.J., 3rd ed.
- [11] Chen, M. M., —1990—, “Scales, similitude, and asymptotic considerations in convective heat transfer,” *Annual Review of Heat Transfer*, C. L. Tien, ed., vol. 3, Hemisphere Pub. Corp., New York, first ed., pp. 233–291.
- [12] Kline, S. J., —1986—, *Similitude and Approximation Theory*, Springer-Verlag, New York.
- [13] Rivas, D. and Ostrach, S., —1992—, “Scaling of low-prandtl-number thermocapillary flows,” *International Journal of Heat and Mass Transfer*, **35**(6), pp. 1469–1479.
- [14] Dantzig, J. A. and Tucker, C. L., —2001—, *Modeling in materials processing*, Cambridge University Press, Cambridge, England ; New York.
- [15] Kou, S., —1996—, *Transport phenomena and materials processing*, Wiley, New York.
- [16] Poirier, D. R. and Geiger, G. H., —1994—, *Transport phenomena in materials processing*, Minerals, Metals & Materials Society, Warrendale, Pa.
- [17] Szekely, J. and Themelis, N. J., —1971—, *Rate phenomena in process metallurgy*, Wiley-Interscience, New York,.
- [18] Segel, L. A., —1972—, “Simplification and scaling,” *SIAM Review*, **14**(4), pp. 547–571.
- [19] Dyke, M. V., —1975—, *Perturbation Methods in Fluid Mechanics*, The Parabolic Press, Stanford, CA, annotated ed.

- [20] Bender, C. M. and Orszag, S. A., —1978—, *Advanced Mathematical Methods for Scientists and Engineers*, International series in pure and applied mathematics, McGraw-Hill, New York, first ed.
- [21] White, R. B., —2005—, *Asymptotic analysis of differential equations*, Imperial College Press, London.
- [22] Kruskal, M. D., —1963—, “Asymptotology,” *Mathematical Models in Physical Sciences*, S. Drobot, ed., Prentice-Hall, Notre Dame, IN, pp. 17–48.
- [23] Fowler, A. C., —1997—, *Mathematical models in the applied sciences*, Cambridge texts in applied mathematics, Cambridge University Press, Cambridge ; New York, NY, USA.
- [24] I. V. Andrianov, L. I. M. and Hazewinkel, M., —2003—, *Asymptotology : ideas, methods, and applications*, Kluwer Academic Publishers, Boston.
- [25] Gell-Mann, M., —1985—, “From renormalization to calculability?” *Shelter Island II. Proceedings of the 1983 Shelter Island Conference on Quantum Field Theory and Fundamental Problems of Physics*, MIT Press, Shelter Island, NY, pp. 3–23.
- [26] Mendez, P. F. and Ordonez, F., —2005—, “Scaling laws from statistical data and dimensional analysis,” *Journal of Applied Mechanics*, **72**(5), pp. 648–657.
- [27] Bruckner, S. and Rudolph, S., —2001—, “Knowledge discovery in scientific data using hierarchical modeling in dimensional analysis,” *SPIE Conference on Data Mining and Knowledge Discovery: Theory, Tools, and Technology*, vol. 4384, Orlando, FL, pp. 208–217.

- [28] Butterfield, R., —1999—, “Dimensional analysis for geotechnical engineers,” *Geotechnique*, **49**(3), pp. 357–366.
- [29] Chen, W.-K., —1971—, “Algebraic theory of dimensional analysis,” *Journal of the Franklin Institute*, **292**(6), pp. 403–422.
- [30] Howard, J. C., —1971—, “Automatic problem formulation using the metric properties of space,” *Journal of the Franklin Institute*, **292**(6), pp. 535–543.
- [31] Mavrovouniotis, M. L., —1997—, “A belief framework for order-of-magnitude reasoning and other qualitative relations,” *Artificial Intelligence in Engineering*, **11**(2), pp. 121–134.
- [32] Weld, D. S. and de Kleer, J., —1990—, *Qualitative Reasoning about Physical Systems*, Morgan Kaufmann Publishers, Inc., San Mateo, CA.
- [33] Weld, D. S., —1990—, “Exaggeration,” *Artificial Intelligence*, **43**(3), pp. 311–368.
- [34] Weld, D. S., —1988—, “Comparative analysis,” *Artificial Intelligence*, **36**, pp. 333–374.
- [35] Mavrovouniotis, M. L. and Stephanopoulos, G., —1988—, “Formal order-of-magnitude reasoning in process engineering,” *Computers & Chemical Engineering*, **12**(9-10), pp. 867–880.
- [36] Raiman, O., —1986—, “Order of magnitude reasoning,” *AAAI-86, Fifth National Conference on Artificial Intelligence*, American Association for Artificial Intelligence, Philadelphia, PA, pp. 100–104.

- [37] de Kleer, J. and Bobrow, D. G., —1984—, “Qualitative reasoning with higher order derivatives,” *Proceedings of AAAI-84*, Austin, TX, pp. 86–91.
- [38] Yip, K. M. K., —1996—, “Model simplification by asymptotic order of magnitude reasoning,” *Artificial Intelligence*, **80**(2), pp. 309–348.
- [39] Mendez, P. F., —1999—, *Order of Magnitude Scaling of Complex Engineering Problems, and its Application to High Productivity Arc Welding*, Doctor of philosophy, Massachusetts Institute of Technology.
- [40] Barenblatt, G. I., —2003—, *Scaling*, Cambridge texts in applied mathematics, Cambridge University Press, Cambridge.
- [41] Barenblatt, G. I., —1996—, *Scaling, Self-Similarity, and Intermediate Asymptotics*, Cambridge texts in applied mathematics, Cambridge University Press, New York, 1st ed.
- [42] Tsung Na, Y. and Hansen, A. G., —1971—, “Similarity analysis of differential equations by lie group,” *Journal of the Franklin Institute*, **29**(6), pp. 471–489.
- [43] Ruark, A., —1935—, “Inspectional analysis: A method which supplements dimensional analysis,” *Journal of the Mitchell Society*, **51**, pp. 127–133.
- [44] Buckingham, E., —1914—, “On physically similar systems; illustrations of the use of dimensional equations,” *Physics Review*, **4**(4), pp. 345–376.
- [45] Waclaw Kasprzak, B. L. and Rybaczuk, M., —1990—, *Dimensional analysis in the identification of mathematical models*, World Scientific, Singapore.

- [46] Sedov, L. I., —1959—, *Similarity and Dimensional Methods in Mechanics*, Academic Press, New York, fourth ed.
- [47] Drobot, S., —1953—, “On the foundations of dimensional analysis,” *Studia Mathematica*, **14**, pp. 84–99.
- [48] Langhaar, H. L., —1951—, *Dimensional Analysis and Theory of Models*, John Wiley & Sons, New York, NY, first ed.
- [49] Szirtes, T. and Rzsá, P., —1997—, *Applied Dimensional Analysis and Modeling*, McGraw Hill, New York.
- [50] Barr, D. I. H., —1987—, “Consolidation of basics of dimensional analysis,” *Journal of engineering Mechanics*, **110**(9), pp. 1357–1376.
- [51] Mendez, P. F. and Eagar, T. W., —2001—, “The matrix of coefficients in order of magnitude scaling,” *Fourth International Workshop on Similarity Methods*, University of Stuttgart, Stuttgart, Germany, pp. 51–67.
- [52] Lin, C. C. and Segel, L. A., —1974—, *Mathematics applied to deterministic problems in the natural sciences*, Macmillan, New York,.
- [53] Sen, A. K. and Davis, S. H., —1982—, “Steady thermocapillary flows in two-dimensional slots,” *Journal of Fluid Mechanics*, **121**, pp. 163 – 186.
- [54] Strani, M., Piva, R., and Graziani, G., —1983—, “Thermocapillary convection in a rectangular cavity: asymptotic theory and numerical simulation,” *Journal of Fluid Mechanics*, **130**, pp. 347 – 376.

- [55] Oreper, G. M. and Szekely, J., 1984, "Heat and fluid flow phenomena in weld pools," *Journal of Fluid Mechanics*, **147**, pp. 53–79.
- [56] Debroy, T. and David, S. A., 1995, "Physical processes in fusion-welding," *Reviews of Modern Physics*, **67**(1), pp. 85–112.
- [57] Wei, P. S. and Liu, H. J., 2012, "Scaling thermocapillary weld pool shape and transport variables in metals," *Welding Journal*, **91**(7), pp. 187s–194s.
- [58] Sahoo, P., DebRoy, T., and McNallan, M. J., 1988, "Surface tension of binary metal-surface active solute systems under conditions relevant to welding metallurgy," *Metallurgical Transactions B*, **19B**, pp. 483–491.
- [59] Mendez, P. F. and Eagar, T. W., 2003, "Penetration and defect formation in high-current arc welding," *Welding Journal*, **82**(10), pp. 296S–306S.
- [60] Mendez, P. F., 2011, "Synthesis and generalisation of welding fundamentals to design new welding technologies: status, challenges and a promising approach," *Science And Technology Of Welding And Joining*, **16**(4), pp. 348–356.
- [61] Tello, K. E., 2009, *Coupled model of heat transfer and plastic deformation for friction stir welding using scaling analysis*, M.s., Colorado School of Mines.
- [62] Duman, U., 2009, *Modeling of Weld Penetration in High Productivity GTAW*, Ph.d., Colorado School of Mines.
- [63] Wypych, G., 2001, *Handbook of Solvents*, ChemTec Publishing.

- [64] Mills, K. C., 2002, *Recommended values of thermophysical properties for selected commercial alloys*, Woodhead, Cambridge.
- [65] Tsai, M. C. and Kou, S., 1989, “Marangoni convection in weld pools with a free surface,” *International Journal for Numerical Methods in Fluids*, **9**, pp. 1503–1516.
- [66] Mendez, P. F. and Eagar, T. W., Year, “Magnitude scaling of free surface depression during high current arc welding,” *Trends in Welding Research, Proceedings of the 5th International Conference*, ASM International, Pine Mountain, GA, pp. 13–18.
- [67] Mendez, P. F. and Eagar, T. W., 2001, “Estimation of the characteristic properties of the weld pool during high productivity arc welding,” *Mathematical Modelling of Weld Phenomena 5*, H. Cerjak and H. K. D. H. Bhadeshia, eds., Institute of Materials, London, UK, pp. 67–94.
- [68] Mendez, P. F., Tello, K. E., and Gajapathi, S. S., Year, “Generalization and communication of welding simulations and experiments using scaling analysis,” *Trends in Welding Research*, ASM International, Chicago, IL.

A Notation for OMS

A.1 Naming convention for vectors and matrices

$\{\dots\}$ column vector; for example, $\{P\}$ indicates the column vector of parameters.

(\dots) column vector of logarithms; for example, (P) indicates a column vector in which each element is a logarithm of the corresponding element of $\{P\}$. The implementation of OMS is independent of the base chosen for the logarithms.

$[\dots]$ matrix; for example, the matrix of coefficients defined in Section 2.1 has the symbol $[C]$

$[\dots]_{\text{cols}}$ submatrix based on the set of columns indicated by the subscript. For example, the matrix of normalized coefficients $[N]$ can be divided into three submatrices $[N]_K$, $[N]_P$, and $[N]_S$ in which each submatrix is formed with the columns of $[N]$ corresponding to the numerical constants K , the parameters P or the unknowns S . Using this notation facilitates matrix operations such as

$$[N] \begin{Bmatrix} (K) \\ (P) \\ (S) \end{Bmatrix} = [N]_K(K) + [N]_P(P) + [N]_S(S)$$

$[\dots]_{\text{rows}}$ submatrix based on the set of rows indicated by the subscript. The subscript i indicates a dominant input row, the subscript o indicates a dominant output row, and the subscript s indicates a row corresponding to a secondary term. For example, $[N]_o$ is the submatrix of $[N]$ that considers only the rows associated with the dominant output terms.

$[\widehat{\dots}]$ matrix in which the columns corresponding to the unknowns have been replaced by the estimations through the following operation

$$[\widehat{\dots}] = [\dots]_{P'} + [\dots]_S[S]$$

Using the matrix of normalized coefficients as an example:

$$[\widehat{N}] = [N]_{P'} + [N]_S[S]$$

A.2 Subscripts

c estimation of characteristic value after approximating functional dependences on the independent variables (described in detail in [2])

e exact magnitude of a characteristic value

i dominant input

o dominant output

s secondary

A.3 Superscripts

\dots^* normalized quantity

\dots^T transposed vector or matrix

$^k \dots$ magnitude, vector, or matrix corresponding to balance k

A.4 Vectors

set	size	description
$\{C\}$	t	coefficients of governing equations with normalized functions
$\{K\}$	u	numerical constants
$\{N\}$	t	coefficients of the normalized governing equations
$\{N_o\}$	q	dominant output coefficients
$\{N_s\}$	$t - q$	secondary coefficients
$\{P\}$	n	parameters
$\{P'\}$	$u + n$	numerical constants and parameters: $\{P'\} = \{\{K\}\{P\}\}^T$
$\{S\}$	q	unknown characteristic values
$\{U\}$		dependent variables
$\{X\}$		independent variables

A.5 Matrices

matrix	size	description
$[B]$	$q \times 3$	matrix of balances
$[C]$	$t \times (u + n + q)$	matrix of coefficients
$[N]$	$t \times (u + n + q)$	matrix of normalized coefficients
$[N_o]$	$q \times (u + n + q)$	matrix of normalized coefficients of dominant outputs
$[N_s]$	$(t - q) \times (u + n + q)$	matrix of normalized secondary coefficients
$[S]$	$q \times (u + n)$	matrix of scaling factors

B Special considerations in the analysis of self consistency

Three aspects of self-consistency deserve special attention: stiff equations, balances of more than two terms, and “pathological” cases.

B.1 “Pathological” cases of self-consistency

The following example illustrates how a self-consistent answer can provide an incorrect estimation, and how the correct balance of dominant terms can be overlooked. Consider the equations

$$u - av - b = 0 \tag{51}$$

$$u - v = 0 \tag{52}$$

with $a = 0.9$ and $b = 0.1$. The exact solution of these equations is $u = v = 1$. Two balances can be chosen, the first one involving the first and second terms in both equations and the second balance involving the third instead of the second term in the first equation. The first balance is incompatible, and the second is self-consistent, yielding $\hat{u}_c = \hat{v}_c = b = 0.1$, which has a large error. On the other hand, the balance discarded as incompatible was representative of the true dominant terms in the first equation, since the first term has a value of 1, the second of 0.9, and the third of only 0.1. The estimation obtained is accurate in the asymptotic case when the second term of the first equation tends to zero ($0 \leq a < 1$). In this particular example, the neglected coefficient has a value of 90% of the dominant ones, which means that this case is very close to the limit of self consistency.

For the case when $a \geq 1$ there are no self-consistent estimations for this system. It has also been observed in other problems that large errors close to the the limit of self consistency have been associated with a non-existing self-consistent solution for parameter combinations outside the original self-consistent regime. Future research is necessary to explore if the disappearance of self-consistent solutions can be used as a reliable warning sign of a self-consistency problem when the secondary coefficients approach 1.

B.2 Stiff equations

Self-consistent estimations might result in balances in which all highest order derivatives in a given independent variable are multiplied by a small factor, such that if the corresponding term is neglected, the boundary conditions for the system cannot be satisfied. This type of equations are called “stiff, ” and can be interpreted as having two regions, an “inner” region close to the boundary or initial time, and an “outer” far far from it. The inner region is directly affected by the boundary and initial conditions, and in it the highest derivatives cannot be neglected. In the outer region, neglecting the highest derivatives is an acceptable simplification.

B.3 Multiple term balances

A special type of self-consistent balance occurs when one or more of the neglected normalized coefficients do not depend on the problem parameters $\{P\}$; thus, the secondary terms will not tend to zero in the asymptotic case. This occurs when matrix $[\widehat{N}_s]_P$ has a row of zeros. Matrix $[\widehat{N}_s]_P$ refers to the submatrix of $[\widehat{N}_s]$ that relates to the parameters but not the

numerical constants. Multiple-term self-consistent balances must be analyzed individually as indicated in the third stage of OMS in Figure 2.

C Upper bound for number of balances

Because of the combinatorial nature of the OMS procedure, the computation time can be very large. For this reason it is useful to estimate beforehand an upper bound of the number of balances to be computed.

The matrix of coefficients involves p equations, but because there are only $q \leq p$ unknown characteristic values, only q equations can be used in each balance. In some cases, some equations (p_r) must be considered in all balances for the problem to make physical sense. Therefore, the total number of combinations of q equations for the balances is given by:

$$\binom{p - p_r}{q - p_r} \quad (53)$$

In this case, the parentheses indicate a combination. For each equation, the upper bound of the number of balances is given by the combination of the number of coefficients in that equation taken two at a time. Therefore, the total number of balances will always be lesser than or equal to:

$$\binom{p - p_r}{q - p_r} \binom{t_{max}}{2}^q \quad (54)$$

where t_{max} is the maximum number of coefficients in any equation considered in the problem.

Equation 54 shows that the upper bound for the number of balances grows in a polynomial way with the number of equations and with the number of terms, and in an exponential way

with the number of unknowns. In OMS the numbers of equations and unknowns do not need to be the same; since OMS provides only a characteristic value, OMS' requisite is that the number of equations is the same or more than the number of unknowns.

For the thermocapillary flow example, $q = 4$, $p = 6$, $t_{max} = 5$, yielding an upper-bound number of combinations of 150,000. The actual number of combinations was 2,486.

D Derivation of Matrix Operations

After Step 4 of the typical scaling procedure detailed in Table 1, a governing equation of the form of Equation 1 can be expressed as:

$$f_i^* (\{X^*\}, \{U^*\}, \{P\}) + N_o f_o^* (\{X^*\}, \{U^*\}, \{P\}) + \sum_j N_{s,j} f_j^* (\{X^*\}, \{U^*\}, \{P\}) = 0 \quad (55)$$

where $f_i^* (\{X^*\}, \{U^*\}, \{P\})$, $f_o^* (\{X^*\}, \{U^*\}, \{P\})$, and $f_s^* (\{X^*\}, \{U^*\}, \{P\})$ are the normalized functions associated with the input term assumed as dominant, output term assumed as dominant, and other terms assumed as secondary in the balance. The normalized coefficients N_o and $N_{s,j}$ correspond to the dominant output and the secondary terms. Without losing generality, in OMS the governing equations are normalized by the coefficient of the input term assumed as dominant; therefore, that term has a coefficient of exactly 1.

Solving for N_o for each of q governing equations and taking logarithms on both sides, the following expression is obtained:

$$\begin{pmatrix} N_{o_1} \\ \vdots \\ N_{o_q} \end{pmatrix} = \begin{pmatrix} -\frac{f_{i_1}^*({X^*}, {U^*}, {P})}{f_{o_1}^*({X^*}, {U^*}, {P})} - \sum_j N_{s_1,j} \frac{f_{s_1,j}^*({X^*}, {U^*}, {P})}{f_{o_1}^*({X^*}, {U^*}, {P})} \\ \vdots \\ -\frac{f_{i_q}^*({X^*}, {U^*}, {P})}{f_{o_q}^*({X^*}, {U^*}, {P})} - \sum_j N_{s_q,j} \frac{f_{s_q,j}^*({X^*}, {U^*}, {P})}{f_{o_q}^*({X^*}, {U^*}, {P})} \end{pmatrix} \quad (56)$$

In this equation $(N_{o_1} \dots N_{o_q})^T$ is a subset of the column vector (N) ; this subset will be called (N_o) . Using the notation of Equation 4 results in

$$(N_o) = [N_o] \begin{Bmatrix} (K) \\ (P) \\ (S) \end{Bmatrix} \quad (57)$$

where $[N_o]$ is a matrix formed by the rows of matrix $[N]$ that correspond to the dominant output terms in the selected q governing equations. Matrix $[N_o]$ can also be divided in two submatrices, such that one submatrix relates to the known numerical constants and parameters, and the other submatrix relates to the unknown characteristic values:

$$[N_o] = [[N_o]_{P'}, [N_o]_S] \quad (58)$$

where $[N_o]_{P'}$ contains the columns of $[N_o]$ that multiply by the known numerical constants and parameters, and $[N_o]_S$ contains the columns that multiply the unknown characteristic values. This way

$$(N_o) = [N_o]_{P'}(P') + [N_o]_S(S) \quad (59)$$

The combination of Equation 56 with Equation 59 results in:

$$[N_o]_{P'}(P') + [N_o]_S(S) = \begin{pmatrix} -\frac{f_{i_1}^*({X^*}, \{U^*\}, \{P\})}{f_{o_1}^*({X^*}, \{U^*\}, \{P\})} - \sum_j N_{s1,j} \frac{f_{s1,j}^*({X^*}, \{U^*\}, \{P\})}{f_{o_1}^*({X^*}, \{U^*\}, \{P\})} \\ \vdots \\ -\frac{f_{i_q}^*({X^*}, \{U^*\}, \{P\})}{f_{o_q}^*({X^*}, \{U^*\}, \{P\})} - \sum_j N_{sq,j} \frac{f_{sq,j}^*({X^*}, \{U^*\}, \{P\})}{f_{o_q}^*({X^*}, \{U^*\}, \{P\})} \end{pmatrix} \quad (60)$$

where $[N_o]_{P'}$ is the submatrix of $[N]$ associated with the dominant output terms, the numerical constants, and the parameters, $[N_o]_S$ is the submatrix of $[N]$ associated with the dominant output terms and the unknown characteristic values, (P') is the combined set of logarithms of the numerical constants and parameters, and (S) is the set of logarithms of the unknown characteristic values, $f_{i_k}^*({X^*}, \{U^*\}, \{P\})$ and $f_{o_k}^*({X^*}, \{U^*\}, \{P\})$ are the normalized forms of the functions associated with the dominant input and dominant output of the k th of q equations considered in the balance. $N_{sk,j}$ and $f_{sk,j}^*({X^*}, \{U^*\}, \{P\})$ are the coefficient and associated function of the j th secondary term in the k th equation; the parentheses indicate that a logarithm operation is applied elementwise. This equation is an exact reformulation of the governing equations. Equation 60 can be simplified by considering only the location of the characteristic value of the dominant terms ($X_{c_k}^*$ for equation k).

Thus:

$$[N_o]_{P'}(P') + [N_o]_S(S) = \begin{pmatrix} -\frac{f_{i_1}^*({X_{c_1}^*}, \{U^*\}, \{P\})}{f_{o_1}^*({X_{c_1}^*}, \{U^*\}, \{P\})} - \sum_j N_{s1,j} \frac{f_{s1,j}^*({X_{c_1}^*}, \{U^*\}, \{P\})}{f_{o_1}^*({X_{c_1}^*}, \{U^*\}, \{P\})} \\ \vdots \\ -\frac{f_{i_q}^*({X_{c_q}^*}, \{U^*\}, \{P\})}{f_{o_q}^*({X_{c_q}^*}, \{U^*\}, \{P\})} - \sum_j N_{sq,j} \frac{f_{sq,j}^*({X_{c_q}^*}, \{U^*\}, \{P\})}{f_{o_q}^*({X_{c_q}^*}, \{U^*\}, \{P\})} \end{pmatrix} \quad (61)$$

Equation 60 involves functions of the independent variables and Equation 61 involves

only one point in the domain for each equation. When the normalization is correct, all functions f^* have a characteristic value ≈ 1 ; therefore, in the asymptotic limit, all secondary terms tend to zero ($N_{s_{k,j}} \rightarrow 0$), resulting in the following simplified form of Equation 61:

$$[N_o]_{P'}(P') + [N_o]_S(\widehat{S}) = 0 \tag{62}$$

where (\widehat{S}) is the estimate of (S) when the secondary terms are neglected.